Environmental Science & Technology

Article

pubs.acs.org/est

The Interplay Between Bioenergy Grass Production and Water Resources in the United States of America

Yang Song,[†] Matthew Cervarich,[†] Atul K. Jain,[*,†] Haroon S. Kheshgi,[‡] William Landuyt,[‡] and Ximing Cai[§]

[†]Department of Atmospheric Sciences University of Illinois, Urbana, Illinois 61801, United States

[‡]ExxonMobil Research and Engineering Company, Annandale, New Jersey 08801, United States

[§]Department of Civil and Environmental Engineering, University of Illinois, Urbana, Illinois 61801, United States

Supporting Information

ABSTRACT: We apply a land surface model to evaluate the interplay between potential bioenergy grass (Miscanthus, Cave-in-Rock, and Alamo) production, water quantity, and nitrogen leaching (NL) in the Central and Eastern U.S. Water use intensity tends to be lower where grass yields are modeled to be high, for example in the Midwest for Miscanthus and Cave-in-Rock and the upper southeastern U.S. for Alamo. However, most of these regions are already occupied by crops and forests and substitution of these biome types for ethanol production implies trade-offs. In general, growing Miscanthus consumes more water, Alamo consumes less water, and Cave-in-Rock consumes approximately the same amount of water as existing vegetation. Bioenergy grasses can maintain high productivity over time, even in water limited regions, because their roots can grow deeper and extract the water from the deep, moist soil layers. However, this may not hold where there are frequent and intense drought events, particularly in regions with shallow soil depths. One advantage of bioenergy grasses is that they mitigate nitrogen leaching relative to row crops and herbaceous plants when grown without applying N fertilizer; and bioenergy grasses, especially Miscanthus, generally require less N fertilizer application than row crops and herbaceous plants.

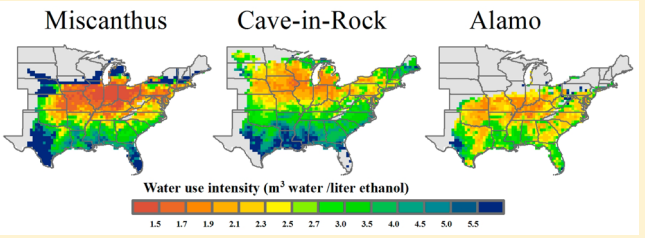

1. INTRODUCTION

Mitigation of anthropogenic climate change motivates interests in the expansion of bioenergy, including the production of ethanol for transportation fuels in the U.S. Corn has been the dominant feedstock, which raises issues regarding land use,[1] food-for-fuel,[2] life-cycle carbon (C) emissions,[3] and other environmental effects such as nitrogen (N) runoff.[4] The use of cellulose to produce ethanol has not achieved a significant scale to date. Yet the production of cellulosic feedstocks is often assumed to perform better than corn with higher yields on land not suitable for agriculture,[1] and less N runoff - although cellulosic feedstocks may consume more water than corn.[5]

Perennial grasses, such as *Miscanthus* × *giganteus Greef et Deu.* (hereafter Miscanthus) and *Panicum viragatum* (hereafter switchgrass), have been identified as potential alternatives for corn in the U.S. due to their low input demand and high biomass productivity.[6−8] Previous studies suggest climate variability, water quantity, and soil nutrient levels control biomass productivity of perennial grasses.[9−14] There is a growing concern that expanding the spatial scale of biofuel feedstocks is likely to decrease water quantity through increased consumption of water due to the vegetation structure, morphology, and physiological properties of these grasses.[15−17]

Water quality, specifically due to nitrogen leaching (NL), is expected to be affected by changes in land cover due to the production of biofuel feedstocks, which necessitates a change in agricultural inputs such as nitrogen fertilizers and may affect nutrient and sediment loads to water bodies.[5,18] To ensure the production of emerging perennial grasses is sustainable, the interplay between bioenergy grass production, water quantity, and N leaching must be understood.

Several studies have examined the implications of growing bioenergy crops on water quantity and water quality in the U.S.. These studies have focused either on a particular site,[5,15,17,19−26] a watershed,[18,27−31] or a small region.[16,32−36] According to these studies, the impacts of growing bioenergy crops on water quantity and NL mainly depend on the location, existing land cover type, and N fertilizer application amount.

Studies in the southern Midwest suggest that growing Miscanthus/switchgrass on crop land (corn/soybean), might have greater water use efficiency (WUE),[14,15,21,34] decreased N leaching (NL) and therefore decreased riverine nitrate load, but increased water consumption.[5,18,26,27] Overall, converting large areas of corn to Miscanthus/switchgrass could improve water quality but reduce surface water availability through decreased local streamflow in the southern Midwest.[17] However, studies in the northern Midwest (e.g., Michigan)[22,23] suggest Miscanthus/switchgrass has higher WUE than row crops;[23] these energy crops have negligible impact on water balance.[22,23]

Received: October 24, 2015
Revised: January 25, 2016
Accepted: February 11, 2016

DOI: 10.1021/acs.est.5b05239
Environ. Sci. Technol. XXXX, XXX, XXX−XXX

In addition to spatial variability in water consumption in the Midwest, studies also suggest that evapotranspiration (ET) depends on precipitation patterns. For example, studies,[5,15,17] show a higher ET for switchgrass than corn during the dry years in IL, but almost the same magnitude of ET for corn and switchgrass during the year with normal precipitation patterns.

Studies suggest that quantitative estimates of NL as a result of growing Miscanthus/switchgrass on grasslands and croplands highly varies with the intensity of N fertilizer application.[5,18,24,26,27,29−31]

While the results for water quantity vary widely among different studies across the U.S. due to temporal and spatial differences in biomass yield patterns, the ethanol productivity (EP) is influenced by changes in soil water quantity, due to changes in phenology, C allocation, and structural development of bioenergy grasses.[37,38] For example, if the growth of bioenergy grasses depletes available soil water, bioenergy grasses may attempt to mitigate its water stress by allocating more C to growing roots toward deeper and moister soil layers.[39] This water-EP feedback has a potential to mitigate the water limiting effect on EP, but simultaneously root growth may come at the cost of shoot growth. Currently, the effect of this feedback on the amount of biomass available for EP is uncertain. Previous modeling studies have not included adaptability of the crops to environmental stresses, thus not fully accounting for the water-EP feedback.[40]

The objective of this study is to evaluate the complex interaction between the production of bioenergy grasses, water quantity and NL across the eastern and central U.S. while accounting for the feedback effects of not only the spatial and temporal characteristics of environmental variables, but also progressive water-EP feedbacks. We expect the outcome of this study to support scientifically sound national policy decisions on bioenergy development especially with regards to cellulosic grasses. To accomplish our objective, we apply an integrated model-data framework, the Integrated Science Assessment Model (ISAM)[12,41−43] to simulate the dynamic growth patterns of bioenergy grasses (e.g., C allocation, vegetation structure, and phenology.). This dynamic approach inherently accounts for the impact of temporal and spatial climate variability, water quantity and NL.[12,43] Our analysis is focused on four spatial zones[12] across central and eastern U.S., which are characterized by their average yield amplitude and temporal yield variance (or stability) over 2001−2012. Specifically, this study evaluates three factors important to producing bioenergy feedstocks in each yield zone: (1) the potential demand of land and water use intensity on a per unit of ethanol production basis, (2) the progressive interaction between water quantity and biomass feedstock production over time, and (3) the spatial changes in soil water quantity and NL as a result of producing bioenergy grasses relative to the existing land cover (e.g., row crops, herbaceous plants, and forests).

2. MATERIALS AND METHODS

2.1. Model Description and Extensions. *2.1.1. General Description.* To accomplish the objectives of this study ISAM has been employed and improved upon. ISAM is a coupled biogeochemical and biogeophysical model with 0.5° × 0.5° spatial resolution and multiple temporal resolutions ranging from half-hour to yearly time steps[12,41,43−45] and calculates terrestrial C, N, water and energy fluxes (e.g., evapotranspiration) through the soil-vegetation-atmosphere system. ISAM accounts for 22 natural plant function types (PFTs) and 5 specific food/bioenergy crops, including corn, soybean, Miscanthus, and two cultivars of switchgrass, Cave-in-Rock, and Alamo.[12,43] Each land grid cell of the model is occupied by a combination of fractional PFTs, including primary and secondary temperate and boreal deciduous/evergreen forests, C3 and C4 grasslands, shrubland, C3 and C4 pastureland, C3 and C4 crops. The historical data for land cover and land use change (LCLUC) for our study time period (1999−2012) is taken from ISAM-HYDE land cover data,[46] which is based on the HYDE 3.1 reconstruction for cropland and pastureland transitions,[47] and wood harvest from FAO (specifically, we include three types of wood harvest from land-use harmonization database that are provided as fractional area of each grid cell: wood harvest from primary forested land, mature secondary forested land, and young secondary forested land). When the model is run for the bioenergy grasses, the existing vegetation in each model grid cell is replaced by the bioenergy crop, as described in Section 2.2. The changes in existing land cover (i.e., replacement of the existing vegetation by prescribed bioenergy grasses) and its effects on water and energy balance, and C and N cycles can be calculated through fully coupled biogeophysical and biogeochemical processes in the model.

2.1.2. Model Extensions. Brief descriptions of biogeophysical and biogeochemical components can be found in the Supporting Information (SI) Section 1. Here we briefly discuss the processes added to these two components of the model for the present study.

ISAM's biophysical component used in the previous studies assumed unrealistic distribution of bedrock depth, which extends up to 3.5m depths globally, and overestimates soil water in certain regions (Figure S2, ISAM-Original case). Here, we implement the bedrock depth distribution based on conterminous USA multilayer soil characteristics data set (CONUS-SOIL)[48] (SI Section 1.1). In addition, we also account for soil structure effect on the thermal and hydrological properties of soils[49] by assuming that root growth alters soil structure and thus changes soil hydraulic conductivity and the minimum suction, mainly in fine-textured soils (SI Section 4.1), because fine-textured soils have microspores, which are usually found in structural aggregate.

To better simulate N availability and its impact on biomass yields for bioenergy crops, we implement the model biological N fixation (BNF) by Miscanthus, temporally varied N demand for per unit of carbon assimilation and spatially varied N translocation rate for three bioenergy grasses (SI Section 4.2).

2.2. Study Region and Model Simulations. This study aims to assess the interaction between biomass production of bioenergy grasses and water quantity and N leaching in the central and eastern U.S. (see Figure S1). We selected this region based on the survival rates of three energy grasses,[50] which depend upon the latitude-of-origin and their varied adaptability to edaphic conditions, such as winter hardiness, day length, heat, dry and cold conditions etc.[12]

We performed four model simulations over the time period of 1999−2012. The first two years of each simulation are the establishment years when both biomass feedstocks and water fluxes are unstable. Therefore, model results are analyzed for the period 2001−2012. The base case model simulation, $ISAM_{veg}$, is carried out over the entire research domain with existing vegetation types (e.g., forest, herbaceous plants, row crops, etc.) in each 0.5° × 0.5° grid cell and calculate the carbon, energy and water fluxes. In three additional model simulations we replace existing vegetation types assumed in

DOI: 10.1021/acs.est.5b05239
Environ. Sci. Technol. XXXX, XXX, XXX−XXX

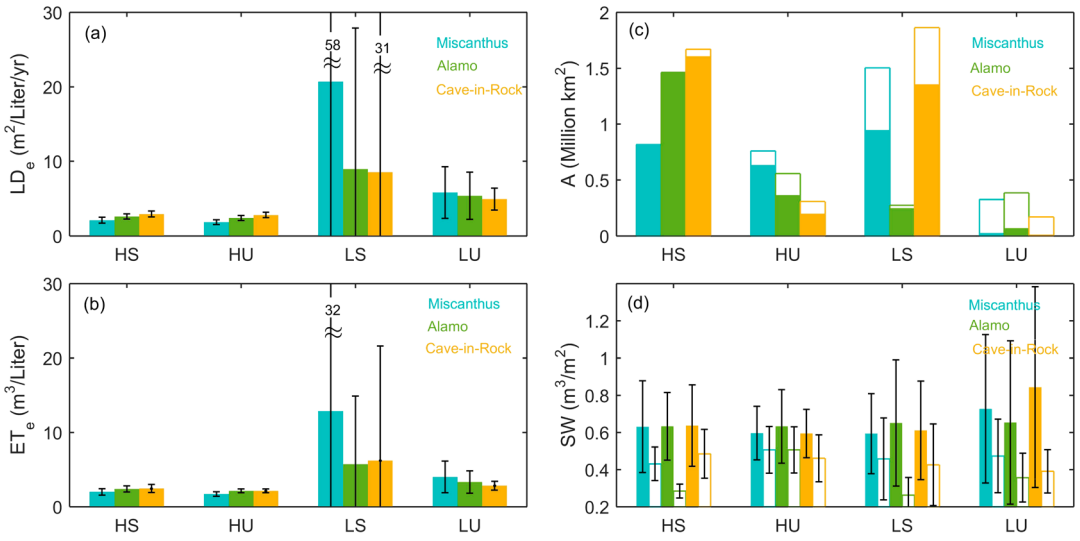

Figure 1. (a) Land demand for producing per unit of ethanol production (LD_e); (b) water use intensity due to producing per unit of ethanol (ET_e), (c) areas for water stressed (portion of bar filled with no color) and water unstressed regions (portion of bar filled with color) (A); and (d) annual mean soil water (SW) for water stressed (bar filled with no color) and water unstressed region (bar filled with color) for three bioenergy grasses (Miscanthus, Cave-in-Rock, and Alamo) in four yield zones: HS: High-Stable, HU: High-Unstable, LS: Low-Stable, and LU: Low-Unstable. Error bars shown are standard deviation (SD) of all grid cell values within each yield zone.

$ISAM_{veg}$ with one type of energy crop at a time: Miscanthus ($ISAM_m$), Alamo ($ISAM_a$) and Cave-in-Rock ($ISAM_c$). The results are presented in Section 3.3 as differences (Δ) in water fluxes between $ISAM_m/ISAM_c/ISAM_a$ and $ISAM_{veg}$. The seedling/rhizome, irrigation and N fertilization rates applied in each model simulation are described in Table S6. We applied the N fertilizers only for the row crops in $ISAM_{veg}$ case, but not for bioenergy crops in $ISAM_m$, $ISAM_a$ and $ISAM_c$, because N fertilizer application rates with time and location for bioenergy crops are highly uncertain[51,52] (See further discussion in Section 4.1.1).

Each model simulation is driven by hourly climate data from NLDAS climate database.[53] The soil texture data is specified based on the State Soil Geographic Database.[54] Before performing model simulations, we first spin up the model to bring soil moisture, temperature, and soil C and N contents to a steady-state using the procedure discussed in SI Section 3.

2.3. Estimates of Biomass Yields and Spatial Yield Zones. The biomass yields for energy crops are calculated using ISAM which accounts for dynamic crop growth processes specific for energy grasses, including phenology development, dynamic carbon allocation, vegetation structure and root distribution, and different removal rates for fresh and old standing brown leaves.[12] The estimated yields are converted to aboveground dry biomass by dividing accumulated aboveground carbon (the sum of leaf and stem carbon) by carbon content in the dry biomass. Unlike row crops, which are planted and harvested every year, bioenergy grasses are planted only in year 1999 and aboveground biomass is harvested each year during the late winter.

Using the method discussed in our previous study,[12] we divide the total growing area for each energy grass into four spatial yield zones characterized by modeled average yield amplitude and temporal yield variance over the period 2001–2012: High-Stable (HS), High-Unstable (HU), Low-Stable (LS) and Low-Unstable (LU) (Figure S9j–l).

Due to model extensions (see Section 2.1.2), the estimated yields and the areas for the four yield zones differ slightly as compared to the results presented in our previous study.[12] In particular, Miscanthus and Cave-in-Rock yields have slightly increased, whereas Alamo yields have slightly decreased in the N-limited southern U.S., where improvements in N dynamic better capture N availability and its effect on bioenergy grass yields (Figure S9a–f). HS and HU zones for Miscanthus and Cave-in-Rock increase at the cost of the decrease in LU zones, whereas HS zone for Alamo slightly decreases at the cost of the increase in area of HU and LU zones (Figure S9g–l). The details of updated modeled averaged yield amplitude and updated distribution of spatial yield zones can be found in SI Section 5.

2.4. Model Calibration and Validation. Previous studies have validated ISAM's ability to simulate C, N, water, and energy fluxes between the atmosphere and the existing current vegetation types and row crops.[43–45] Site level data has also been employed to calibrate and validate the modeled carbon assimilation rates, leaf area index (LAI), aboveground and belowground biomasses, biomass yield for the three bioenergy grasses.[12] ISAM estimated spatial and temporal variability in bioenergy grass biomass yields have been evaluated with observed biomass yields at 17 planting sites for Miscanthus, 28 sites for Cave-in-Rock, and 22 sites for Alamo across the U.S. These sites cover geospatial area of the U.S., ranging from 26.22°N to 46.88°N.

In addition, in this study we evaluated the modeled ET for bioenergy grasses with field measured ET from three sites for Miscanthus, five sites for Cave-in-Rock, and one site for Alamo (Table S5, Figure S1, and SI Section S4.1); soil water content (SW) from 1 site for Miscanthus and 1 site for Cave-in-Rock. In addition, N dynamic effect on bioenergy grasses was evaluated by examining the model's ability to capture the response of observed yields of bioenergy grasses to different levels of N fertilizer application from 15 sites for Miscanthus, 15 sites for Cave-in-Rock and 8 sites for Alamo (Table S5, Figure S1 and Section 4.2 of SI); modeled NL from 7 sites for Miscanthus and 3 sites for Cave-in-Rock (Table S5, Figure S1, and SI Section 4.3.1). Since the model was further extended in

DOI: 10.1021/acs.est.5b05239
Environ. Sci. Technol. XXXX, XXX, XXX–XXX

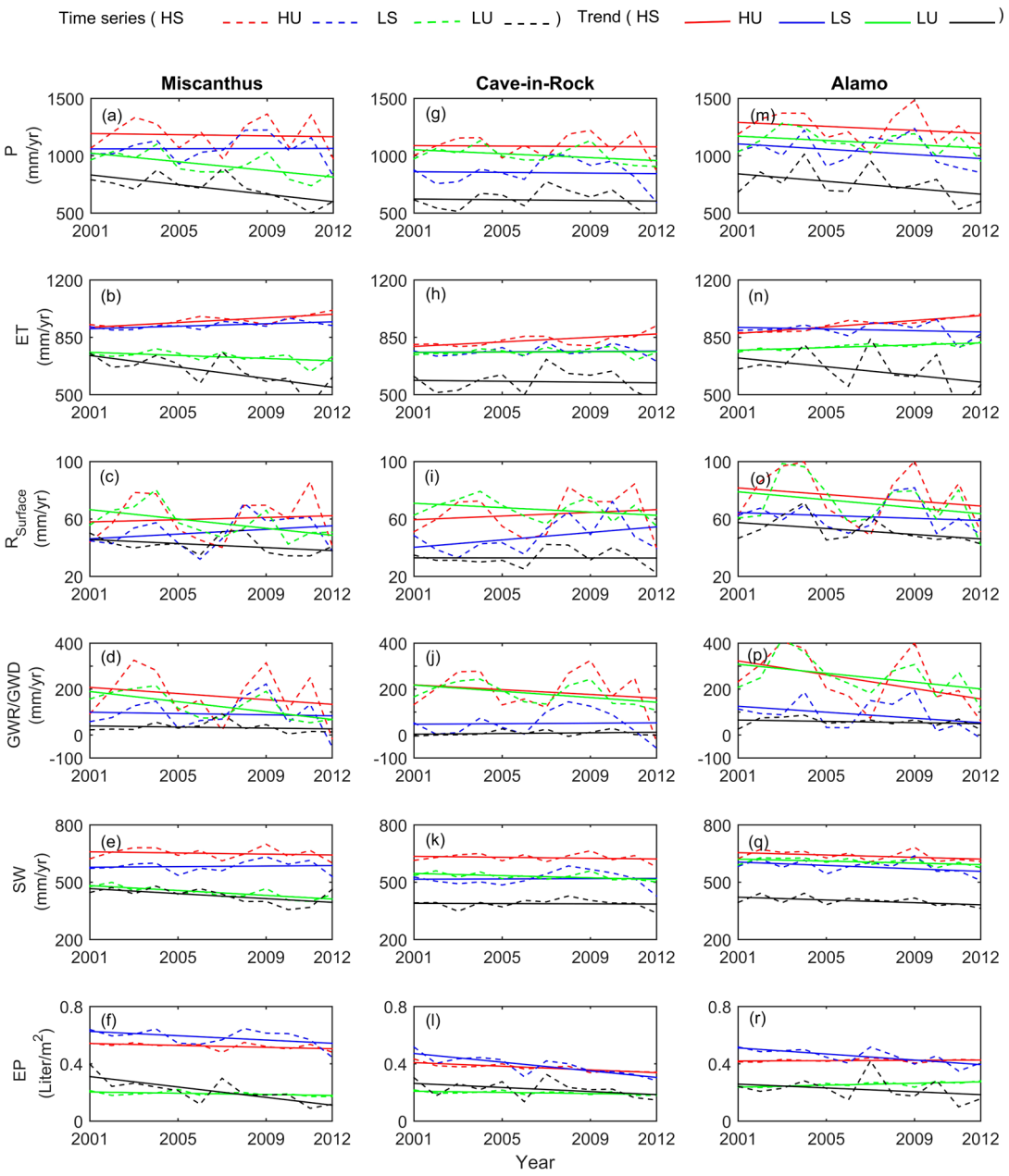

Figure 2. Time series and trends of annual accumulated precipitation (P),[44] evapotranspiration (ET), surface runoff ($R_{surface}$), groundwater recharge/discharge (GWR/GWD) (positive values refers to annual net GWR), soil water storage in entire soil column (SW), and ethanol productivity (EP) calculated based on model for three bioenergy grasses (Miscanthus, Cave-in-Rock and Alamo) in four spatial yield zones: HS: high-stable, HU: high-unstable, LS: low-stable, LU: low-unstable. Values for each variable are averaged values over each yield zone.

this study, ISAM estimated spatial and temporal variability in biomass yields for bioenergy grasses were re-evaluated with measured data (SI Table S1).[12] Overall, the improved ISAM is able to capture seasonal and interannual variability in ET, SW, and NL and bioenergy grasses yields in the study region (SI Figures S2–S8). Our model estimated results for changes in water fluxes at regional scale are also compared with other published modeling studies (See SI Section 6).

3. RESULTS

3.1. Estimates of Land and Water Demand to Grow Bioenergy Grasses. We estimate the potential demand of land (LD_e), defined as the area per unit liter of ethanol, and the potential amount of water use intensity (ET_e), defined as the annual total water evapotranspiration per unit liter of ethanol for producing bioenergy grasses (see SI Section 2 for calculation of LD_e and ET_e). Our results suggest that both LD_e and ET_e have significant differences across the four yield zones. Overall, LD_e in HS and HU zones would be 2–3 m^2 (Figure 1a) and ET_e 1.7–2.5 m^3 (Figure 1b), which are about 57–90% and 30–80% less than in LU and LS zones (Figure 1a,b).

The LD_e and ET_e for Miscanthus in HS and HU zones are 19–30% and 19–20% lower than that for other two bioenergy grasses (Figure 1a,b). However, the total land to produce Miscanthus in these two high yielding zones is only 1.45 million km^2, which is 21–23% less than two switchgrasses in these two zones (Figure 1c).

DOI: 10.1021/acs.est.5b05239
Environ. Sci. Technol. XXXX, XXX, XXX–XXX

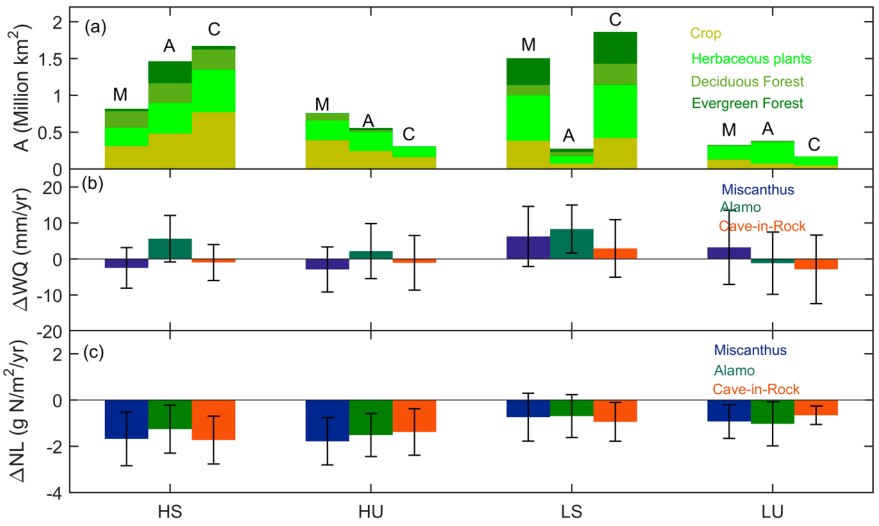

Figure 3. (a) Total area of each existing vegetation type (A), (b) change in annual total (soil and unconfined aquifer) water quantity change (ΔWQ) and (c) change in annual Nitrogen leaching (ΔNL). The change (Δ) in panels (b) and (c) represents the difference between each energy grass model simulation ($ISAM_m$, $ISAM_c$, $ISAM_a$) and base model simulation case ($ISAM_{veg}$). The values plotted are the average values for the time period 2001−2012. In figure (a) stacked bars, M, A, and C, for each zone are for Miscanthus, Alamo, and Cave-in-Rock, respectively. Error bars in panels (b) and (c) show standard deviation (SD) of values of all cell grids within each yield zone.

In each yield zone, we further identify the water limiting area (WLA) to produce bioenergy grasses based on mean water stress over the growing season (see SI Section 2 for the description). Our results indicate that WLAs are mainly located in HU, LU and LS zones (Figure 1c). WLA for Miscanthus in these three zones are about 0.1, 0.3, and 0.6 million km^2 (Figure 1c), whereas the remaining area in each zone is limited by other environmental factors, such as N availability, high/low temperature etc. Miscanthus is primarily water limited in the central and southern Great Plains (Figure S10a). The dominant WLA for Alamo is southern Great Plains in HU (0.2 million km^2) and LU (0.3 million km^2) zones (Figures 1c and S10c). The WLAs for Cave-in-Rock are the Great Plains in HU (0.1 million km^2), LU (0.2 million km^2), and LS (0.5 million km^2) zones (Figures 1c and S10b). On average, the WLAs for switchgrasses have less than 0.45 m^3/m^2 of available SW, whereas Miscanthus can be limited by water up to 0.51 m^3/m^2 of available SW in HU zone (Figure 1d). These results suggest that two switchgrasses have greater tolerance to dry conditions than Miscanthus.

3.2. The Progressive Interaction Between Soil Water and the Production of Biomass Feedstocks. The biomass production of bioenergy grass over its lifetime (10−15 years) with changes in precipitation rates can progressively change the hydrological cycle and thus SW, which depends on the trade-off between precipitation (P), ET, surface runoff ($R_{surface}$) and groundwater flux. The positive (negative) groundwater refers to annual net groundwater recharge (GWR) (discharge, GWD). The higher rates of P may increase $R_{surface}$ and/or GWR, but growing bioenergy grasses increases ET, leading to a decrease in $R_{surface}$ plus GWR (or increase GWD). Also, root growth of bioenergy grasses may change soil structure properties[49] and increase the infiltration of P toward deeper soil layers and increase GWR. These temporal changes in ET, $R_{surface}$, and GWR/GWD finally change SW and thus water stress conditions over time. In addition, the changes in P rates also impact the rate of change for SW, ET, and GWR/GWD over time.[55] The change in SW may in turn impact ethanol productivity (EP) over time, defined here as the ethanol production from bioenergy grasses per unit of land area (see SI Section 2 for its calculation). To evaluate this progressive interaction between SW and EP after the establishment of bioenergy grasses, we analyze trends of annual total P, ET, $R_{surface}$, and GWR/GWD, and annual mean SW and EP over the time period 2001−2012.

While there is no significant change in P rates over the time period 2001−2012 for Miscanthus' HS and HU zones (Figure 2a) and Cave-in-Rock's HS zone (Figure 2g), ET increases at an annual average rate of 3−6 mm yr^{-1} for Miscanthus and 6 mm yr^{-1} for Cave-in-Rock (Figure 2b,h) due to increased transpiration by a greater canopy cover and deeper roots over the same time period. This increased ET first reduces SW, but then compensated by increased GWD (Figure 2d,j), finally leading to no significant effect on SW (Figure 2e,k). However, production of Miscanthus in LS and LU zones (Figure 2e), Cave-in-Rock in LS zone (Figure 2k) and Alamo in HS, HU, and LU zones (Figure 2q) significantly decrease SW over the same period. The decreasing trend for SW for Alamo in HS zone results from decreasing P rates (Figure 2m), increasing ET rates (Figure 2n), and due to SW extraction by deeper growing roots, which also tends to decrease GWR and $R_{surface}$ by 12 mm yr^{-1} and 0.94 mmyr^{-1} respectively (Figure 2i,o,p). Our results suggest that a decreasing trend of P in the water-limiting regions of Miscanthus (LS and LU) and Alamo (HU and LU) (Figure 2a,m) decrease SW (Figure 2e,q) and limit water availability and significantly decrease ET from 2001 to 2012 (Figure 2b,n). The decreasing trends in ET in WLA are lower than the decreasing trends in P, leading to a decreasing of GWR over the same period (Figure 2f,r). These results suggest that production of Miscanthus and Alamo can greatly aggravate groundwater depletion in currently water-limiting areas.

In general, continuous production of bioenergy crops reduces SW and limits EP over time. Our modeling results show that, in certain cases, roots respond to reduced SW by growing toward deeper moist soil layers and partially mitigate the effects of reduced SW. For example, there is no apparent change in modeled EP for Alamo (Figure 2r) in HS zone due to this effect. In contrast, Miscanthus and Cave-in-Rock in LU

DOI: 10.1021/acs.est.5b05239
Environ. Sci. Technol. XXXX, XXX, XXX−XXX

zones and Alamo in HU and LU zones are not able to avail this benefit due to the shallow bedrock depths in these regions, which limit the root growth, leading to progressively enhanced water stress conditions for the grasses. Our results indicate that EP from Miscanthus in LU zone and for Alamo in LU and HU zones can significantly decrease (0.02 Liter m^{-2} yr^{-1} for Miscanthus and 0.01 Liter m^{-2} yr^{-1} for Alamo) (Figure 2f,r). Cave-in-Rock EP in HS and HU zones (Figure 2l) decreases, possibly due to progressive N limitation.[56]

Overall, our results suggest that growing Miscanthus and Alamo in LU zone and Alamo in HU zone would experience enhanced dry conditions over time and limit EP. Growing bioenergy grasses in HS yield zones could decrease total SW over time, but without impacting EP. This is because deeper roots of bioenergy crops could use water from deeper moist soil layers to mitigate water stress conditions under normal climate conditions.

3.3. Water Implication of Producing Bioenergy Grasses on the Existing Vegetation Land. This section discusses the Δ*results* (differences between the bioenergy grass modeling simulations, $ISAM_m$/$ISAM_c$/$ISAM_a$, and the base case, $ISAM_{veg}$) for annual total soil water quantity (WQ = P − ET − R), ET, runoff (R = $R_{surface}$ + $R_{sub\_surface}$, where $R_{surface}$ stands for surface and $R_{sub\_surface}$, subsurface runoff) and NL fluxes over the period 2001−2012. The Δwater fluxes (ΔWQ, ΔET, and ΔR) and ΔNL are then averaged over all grids in each yield zone of the study region. Positive Δfluxes refer to increased water fluxes due to conversion of existing vegetation to the bioenergy grasses. The objective here is to quantify the spatially averaged effects of bioenergy grasses on water quantity and NL when they are grown in area of existing vegetation (row crops, herbaceous plants (e.g., grass, pasture, shrub) and forests) over the period 2001−2012 (see SI Section 2 for the details).

The net effect of replacing row crops (Figure S11a) and herbaceous plants (Figure S11b) with energy grasses on water quantity depends on the trade-off between ET and R. For example, replacing shallow-rooted row crops and herbaceous plants with deep-rooted bioenergy grasses[57−61] could lead to increased ET, but decreased *R*.

Overall, our study finds high yielding zones (HS and HU) for Miscanthus and Cave-in-Rock are primarily consist of crop and herbaceous, but Alamo's HS occupies approximately equal area of crop, herbaceous and forest, whereas HU occupies mainly crop and herbaceous lands (Figure 3a). Growing Miscanthus in HS and HU zones decreases WQ by 2.5 mm yr^{-1} and 2.9 mm yr^{-1}, whereas Alamo production in these two zones increases WQ by 5.6 mm yr^{-1} and 2.2 mm yr^{-1}, respectively (Figure 3b and Table 1).

Growing Cave-in-Rock on croplands and temperate deciduous forests increases WQ, but on grassland decreases WQ (Figure 3a), such as in the southeastern Midwest region in HS and HU (Figure S12d−f). In contrast, productions of three energy crops in LS, which occupies large areas for herbaceous plants and forests, and Miscanthus in LU, which occupies large areas for cropland and forests (Figure 3a), increase WQ due to a larger decrease in ET and smaller increase in R (Table 1). Overall, the maximum increase in WQ is for Alamo in LS of 8.3 mm yr^{-1} (Figure 3b and Table 1).

Our results suggest that producing Miscanthus on all cropland (Figure S11a) can decrease WQ by up to 16 mm yr^{-1} (Figure S12a), except for the northern part of the central Midwest in HS and HU zones (Figure S12a). Cave-in-Rock on cropland decreases WQ by 10 mm yr^{-1} or less, except for in the southern Midwest (Figure S12d). The reduction in WQ with the replacement of row crops by Miscanthus and Cave-in-Rock is because Miscanthus and Cave-in-Rock under favorable environmental conditions can develop larger canopy and deeper root systems than row crops and thus canopy water interception and root water extraction increase, leading to a positive ΔET (Figure S12j,m) and negative ΔWQ for Cave-in-Rock. Unlike Miscanthus and Cave-in-Rock, growing Alamo on the cropland does not decrease WQ, except for in eastern Texas and part of southern Atlantic region (Figure S12g), because negative Δ*ET* (Figure S12p) offsets positive ΔR (Figure S12y). The positive Δ*ET* and negative ΔR with growing Alamo on the cropland and herbaceous is due to N limitation, which constrains the growth of Alamo and thus ET. Modeling results shown in Figure S6 suggests that Alamo productivity is more sensitive to N fertilizer than the productivity of Miscanthus and Cave-in-Rock, indicating that Alamo needs more N fertilizer to maintain high productivity than Miscanthus and Cave-in-Rock. Therefore, growing Alamo without N fertilizer application induces N limitation on the Alamo growth, leading to less Alamo productivity and lower ET and higher R as compared to the case where row-crops are grown with N fertilizer applications.

Similar to growing bioenergy grasses on croplands, growing energy crops on herbaceous lands (Figure S11b) leads to a decrease in WQ by 16 mm yr^{-1} in most area of the Great Plains for the three bioenergy grasses and the central Midwest for Miscanthus and Cave-in-Rock (Figure S12b,e,h) due to increase in ET (Figure S12k,n,q) over a longer growing season and increase in soil evaporation after harvest of bioenergy grasses.[29] Similar to the crops, the loss of soil N in the process of growing Alamo on herbaceous lands introduces a lower ET and higher R for Alamo.

In general, producing bioenergy grasses on temperate evergreen forest, especially in the southeast (Figure S11c),

Table 1. Water Budget Change Due to Growing of Bioenergy Grasses on Existing Vegetation (Crops, Herbaceous Plants and forest) in Each Spatial Yield Zone[a]

bioenergy crop	yield zone	ΔET (mm yr^{-1})	ΔR (mm yr^{-1})	ΔWQ (mm yr^{-1})
Miscanthus	HS	36.0	−33.5	−2.5
	HU	44.3	−41.4	−2.9
	LS	−48.4	42.1	6.3
	LU	−1.4	−1.9	3.2
Alamo	HS	−85.3	79.7	5.6
	HU	−26.0	23.8	2.2
	LS	−107.0	98.7	8.3
	LU	−1.6	2.8	−1.2
Cave-in-Rock	HS	−21.0	22.0	−1.0
	HU	0.5	−0.6	−1.1
	LS	−58.7	55.8	2.9
	LU	5.8	−2.9	−2.9

[a]Here Δ is difference between model simulations for bioenergy crops (ISAMm, ISAMa, ISAMc) and base model simulation case (ISAMveg) for evapotranspiration (ET), runoff (R) and water quantity (WQ, the sum of soil water and unconfined aquifer water) and ΔWQ = ΔET + ΔR. HS, HU, LS, and LU are high and stable, high and unstable, low and stable, low and unstable yield zones. All values in the table are averaged values over each yield zone and for the period 2001−2012.

DOI: 10.1021/acs.est.5b05239
Environ. Sci. Technol. XXXX, XXX, XXX−XXX

increases WQ (Figure S12c,f,i), because (i) smaller canopy of bioenergy grasses withdraws less water through ET than for forests (Figure S12l,o,r); (ii) R increases due to increased throughfall rates; and (iii) water infiltration decreases due to higher WQ for bioenergy grasses than for forests, which further increases R (Figure S12u,x,za). Unlike temperate evergreen forests, production of bioenergy grasses on temperate deciduous forest land (Figure S11c), in general, has no significant impact on WQ, because decreased ET is almost the same as increased R (Figure S12c,f,i).

Our modeling results for NL suggests that production of bioenergy grasses without N fertilizer application in their HS and HU zones decreases NL by around 1.4−2.8 gN m^{-2} yr^{-1}, which is usually higher than the reduction in NL in LU and LS zones (Figure 3c). Our modeling results also suggest a decrease in NL by maximum 2 gN m^{-2} yr^{-1} due to production of bioenergy grasses on the croplands and grasslands in the study regions (Figure S14a,b,d,e,g,h). Finally, our results suggest that growing bioenergy grasses on forest land do not significantly impact NL (Figure S14c,f,i).

Since the NL rates can vary with different N fertilizer application rates, in Section 4.1.1 we further investigate the sensitivity of effects of different nitrogen (N) application rates on our model estimates rates for NL.

4. DISCUSSION

4.1. Limitations and Uncertainties. *4.1.1. Growing Energy Crops with Nitrogen Fertilization Application.* This study suggests that production of energy grasses, particularly when they are grown on herbaceous and row croplands, can mitigate NL based on the assumption that N fertilizer is applied for row crops but not for bioenergy grasses. Our assumption for growing bioenergy crops without N fertilizer applications, as discussed in Section 3.3, is based on the understanding that these crops need to be grown at least cost and with least impact on water quality and N_2O emissions. Energy crops are expected to require minimal fertilizer input, because they recycle nutrients to belowground roots and rhizomes, before the dry shoots are harvested in late fall and early winter.[51] While these crops are highly efficient at extracting soil nutrients, studies also suggest that limited application of N fertilizer may make some bioenergy crops nitrogen stressed and constrain biomass yield production.[56,62,63] Field experiments[24] have also shown a significant increase in NL with N fertilizer input, suggesting that our original assumption of zero N fertilizer rates possibly underestimates ethanol productivity, ET and NL rates in N-limited regions.

Here we perform additional model simulations to assess the response of biomass yield and NL for three bioenergy grasses to N fertilizer application. The N fertilizer application rates for bioenergy grasses for these model simulations are compiled based on previous studies (see detailed description in SI Section 4.3.2), which vary spatially from 20 to 60 kg N $ha^{-1}yr^{-1}$ for Miscanthus, 40−120 kg N $ha^{-1}yr^{-1}$ for two switchgrasses (Figure S13a−c).

Our analysis suggests that model estimated spatial distribution of ΔNL_N (same as ΔNL, but calculated with N fertilizer application) is approximately of the same magnitude as ΔNL when Miscanthus is grown without N fertilizer application (Figure S14a−c, j−l), suggesting that the additional amount of N does not impact Miscanthus NL.

However, NL for two switchgrasses changes spatially due to N fertilizer applications. Our model results show that growing Cave-in-Rock and Alamo with N fertilizer application on the cropland (Figure S14m,p) increases ΔNL_N by 10−50% and 5−100% as compared to their respective ΔNL values. In case of Cave-in-Rock, changes are observed especially in the southern U.S. and the central Great Plains (Figure S14m), whereas for Alamo changes occur mainly in southern Midwest and middle Atlantic region (Figure S14p). Similar as on the cropland, ΔNL_N for two swichgrasses on the herbaceous land is also higher than ΔNL, especially in most of the southern USA region (Figure S14n,q).

Our modeling results suggest that ΔNL on forest land for two switchgrasses almost negligible in study region (Figure S14f−i). However, application of N fertilizer increases ΔNL_N by 1−15 times for Cave-in-Rock and 3−20 times for Alamo as compared to their respective ΔNL values. This is because added N fertilizer amount is leached due to higher ΔR values when switchgrasses are grown on forests (Figure S12,x,za).

Our analysis suggests that assessing the impact of bioenergy grasses production on NL could vary with application of N fertilizer, particularly for two switchgrases. The spatial variability in recommended N fertilization rate needs to be further studied in the future in order to mitigate increased NL with application of N fertilizer for bioenergy grasses.

4.1.2. Model Limitations. This study has made efforts to calibrate and validate the model for various model output variables based on available site-specific observed data within the research domain. Overall, these efforts indicate that the model is able to capture spatial and temporal variability in biomass yield of bioenergy grasses and their responses to N fertilizer over the most of research domain. The model is also able to capture interannual variability in ET and NL fluxes with the growth of Miscanthus and Cave-in-Rock in the Corn-Belt region ranging from 34.90°N to 42.40°N. However, there could be some uncertainty when applying the model to grow these two bioenergy grasses out of the Corn-Belt region due to the limitation of available observed data. In addition, impacts of EP from Alamo on ET and NL across the whole research domain needs to be further assessed when more measured data is available.

Despite accounting for many processes and feedback mechanisms, there remain some important feedback processes, which are not currently considered in our model. In particular, our model has not accounted for the effect of changes in ET on precipitation, although the model accounts for the effect of changes in precipitation patterns on ET. The decrease in ET due to growing bioenergy grasses in forest-dominated region possibly decreases local convective moisture transport and cloud formation, leading to a decrease in precipitation.[64,65] Conversion of row crops to bioenergy grasses possibly increases precipitation and decreases air temperature due to increased ET and higher albedo.[66] The lack of this feedback may result in the overestimation of change in WQ. It is most likely possible that exclusion of some of the important feedbacks may impose limits on the accuracy of model simulated water fluxes. Therefore, we plan to include them in our future work by coupling ISAM land surface model with a regional climate model.

While these modeling limitations impose some limits on the accuracy of simulated water processes, the modeling framework we applied in the present study is a reasonable and powerful tool to study the implications of growing bioenergy crops on water quantity and quality.

DOI: 10.1021/acs.est.5b05239
Environ. Sci. Technol. XXXX, XXX, XXX−XXX

4.2. Maximizing Yield and Minimizing Water Impacts of Bioenergy Grasses. Here we use a well calibrated and validated ISAM land surface model to evaluate the impact of the production of the biomass feedstocks of three different bioenergy grass on water quantity and NL in the central and eastern U.S. First, we reconstructed four yield zones to identify the regions with high ethanol productivity and limited impact on water quantity and NL.

It is important to note that the HS zone is able to maintain high productivity for growing bioenergy grasses over the time period 2001−2012. Although growing Alamo in HS yield zone decreases total SW with time, water extraction from deeper moist soil layers by its roots mitigates water stress conditions under normal climate conditions. However, growing energy crops in two unstable zones (HU and LU) aggravates soil water depletion over time and in turn limits the ethanol productivity.

We identify spatial regions within two high yield zones as "likely", "less likely" and "not likely" to grow each of the three bioenergy crops from the perspective of water impacts (Table S7). Overall, most common "likely" regions are eastern Ohio, eastern Kentucky, eastern Tennessee and the Northern Atlantic regions (Table S7), where growing bioenergy grasses almost has negligible impact on WQ (Figure S12a−i). In addition, compared with Miscanthus and Cave-in-Rock, Alamo has larger likely region within HS zone, which is mostly occupied by forests (Table S7). However, substitution of forest in this region is not recommended, considering other important economic and ecosystem services of forest ecosystem, such as wood products, and carbon sequestration.

The "less likely" regions for Miscanthus and Cave-in-Rock include Missouri, southern Illinois and the Mississippi River watershed regions of eastern Arkansas. (Table S7 and Figure S12a−f). Miscanthus and Cave-in-Rock in these regions deplete more WQ than the existing row crops and herbaceous plants (Figure S12a−f).

In addition, most of the "less likely" and "not-likely" regions for bioenergy grasses are located in the Great Plains region of HU zones (Table S7) due to the fact that drier conditions in this region limit the production of bioenergy grasses.

While HS and HU zones may be able to attain optimal distribution of the three bioenergy grasses in regards to highest EP with limited impacts on water quantity, substitution of existing land cover types (row crops, herbaceous plants and forests) for bioenergy grasses in these two zones may raise other issues involving, food and wood production, C sequestration, land degradation etc., which needs to be studied in future research.

■ ASSOCIATED CONTENT

Supporting Information

The Supporting Information is available free of charge on the ACS Publications website at DOI: 10.1021/acs.est.5b05239.

Details on ISAM model improvement and evaluation for hydrological cycle processes, the model performance of simulating evapotranspiration (ET) for energy crops and their impacts on soil moisture and nitrogen leaching, model spin-up procedure, calculation of assessment metrics, and comparison of model results with other studies (PDF)

■ AUTHOR INFORMATION

Corresponding Author

*Phone: 217-333-2128; fax: 217-244-1752; e-mail: Jain1@illinois.edu.

Notes

The authors declare no competing financial interest.

■ ACKNOWLEDGMENTS

This research was partly supported by the US National Science Foundation (No. NSF-AGS-12-43071), US Department of Energy (DOE) Office of Science (DOE-DE-SC0006706) and a grant from ExxonMobil Research and Engineering Company. We thank Dr. Gregory F. McIsaac and four anonymous reviewers for their valuable comments. We also acknowledge that we have used the ArcGIS database in the manuscript and SI files.

■ REFERENCES

(1) Cai, X.; Zhang, X.; Wang, D. Land Availability for Biofuel Production. *Environ. Sci. Technol.* **2011**, *45* (1), 334−339.

(2) Service, R. F. Biofuel Researchers Prepare To Reap a New Harvest. *Science* **2007**, *315*, 1488−1491.

(3) Davis, S. C.; Anderson-Teixeira, K. J.; DeLucia, E. H. Life-cycle analysis and the ecology of biofuels. *Trends Plant Sci.* **2009**, *3* (14), 140−146.

(4) Demissie, Y.; Yan, E.; Wu, M. Assessing Regional Hydrology and Water Quality Implications of Large-Scale Biofuel Feedstock Production in the Upper Mississippi River Basin. *Environ. Sci. Technol.* **2012**, *46*, 9174−9182.

(5) McIsaac, G. F.; David, M. B.; Mitchell, C. A. Miscanthus and Switchgrass production in Central Illinois: impacts on hydrology and inorganic Nitrogen leaching. *J. Environ. Qual.* **2010**, *39*, 1790−1799.

(6) Gunderson, C. A.; Davis, E. B.; Jager, H. I.; West, T. O.; Perlack, R. D.; Brandt, C. C.; Wullschleger, S. D.; Baskaran, L. M.; Wilkerson, E. G.; Downing, M. E. *Exploring potential U.S. Switchgrass Production for Cellulosic Ethanol Using Empirical Modeling Approaches*; Oak Ridge National Laboratory: Oak Ridge, TN, 2008; ORNL/TM 2007/183.

(7) Heaton, E.; Dohleman, F.; Long, S. Meeting US biofuel goals with less land: the potential of Miscanthus. *Global Change Biol.* **2008**, *14*, 2000−2014.

(8) Lewandowski, I.; Scurlock, J. M. O.; Lindvall, E.; Christou, M. The development and current status of perennial rhizomatous grasses as energy crops in the US and Europe. *Biomass Bioenergy* **2003**, *25*, 335−361.

(9) Behrman, K.; Kiniry, J.; Winchell, M.; Juenger, T.; Keitt, T. Spatial forecasting of switchgrass productivity under current and future climate change scenarios. *Ecol, Appl.* **2013**, *23*, 73−85.

(10) Miguez, F.; Maughan, M.; Bollero, G.; Long, S. Modeling spatial and dynamic variation in growth, yield, and yield stability of the bioenergy crops Miscanthus × giganteus and Panicum virgatum across the conterminous United States. *GCB Bioenergy* **2012**, *4*, 509−520.

(11) Jager, H.; Baskaran, L.; Brandt, C.; Davis, E.; Gunderson, C.; Wullschleger, S. Empirical geographic modeling of switchgrass yields in the United States. *GCB Bioenergy* **2010**, *2*, 248−257.

(12) Song, Y.; Jain, A.; Landuyt, W.; Kheshgi, H.; Khanna, M. Estimates of Biomass Yield for Perennial Bioenergy Grasses in the USA. *BioEnergy Res.* **2015**, *8* (2), 688−715.

(13) Thomson, A.; Izaurralde, R.; West, T.; Parrish, D.; Tyler, D.; Williams, J. *Simulating Potential Switchgrass Production in the United States*; Pacific Northwest National Laboratory: Richland, WA, 2009; PNNL-19072.

(14) Zhuang, Q.; Qin, Z.; Chen, M. Biofuel, land and water: maize, switchgrass or Miscanthus ? *Environ. Res. Lett.* **2013**, *8* (1), 015020 1−6..

(15) Hickman, G.; Vanloocke, A.; Dohleman, F.; Bernacchi, C. A comparison of canopy evapotranspiration for maize and two perennial

DOI: 10.1021/acs.est.5b05239
Environ. Sci. Technol. XXXX, XXX, XXX−XXX

grasses identified as potential bioenergy crops. *GCB Bioenergy* **2010**, *2*, 157−168.
(16) Vanloocke, A.; Bernacchi, C.; Twine, T. The impacts of Miscanthus × giganteus production on the Midwest US hydrologic cycle. *GCB Bioenergy* **2010**, *2*, 180−191.
(17) Le, P.; Kumar; Drewry, D. Implications for the hydrologic cycle under climate change due to the expansion of bioenergy crops in the Midwestern United States. *Proc. Natl. Acad. Sci. U. S. A.* **2011**, *108*, 15085−15090.
(18) Schilling, K.; Jha, M.; Zhang, Y. K.; Gassman, P.; Wolter, C. Impact of land use and land cover change on the water balance of a large agricultural watershed: Historical effects and future directions. *Water Resour. Res.* **2008**, *44*, W00A09 1−12..
(19) Hendrickson, J. R.; Schmer, M. R.; Sanderson, M. A. Water Use Efficiency by Switchgrass Compared to a Native Grass or a Native Grass Alfalfa Mixture. *BioEnergy Res.* **2013**, *6* (2), 746−754.
(20) Wagle, P.; Kakani, V. G. Growing season variability in evapotranspiration, ecosystem water use efficiency, and energy partitioning in switchgrass. *Ecohydrology* **2014**, *7* (1), 64−72.
(21) Zeri, M.; Hussain, M. Z.; Anderson-Teixeira, K. J.; DeLucia, E.; Bernacchi, C. J. Water use efficiency of perennial and annual bioenergy crops in central Illinois. *J. Geophys. Res.: Biogeosci.* **2013**, *118* (2), 581−589.
(22) Abraha, M.; Chen, J.; Chu, H.; Zenone, T.; John, R.; Su, Y.-J.; Hamilton, S. K.; Robertson, G. P. Evapotranspiration of annual and perennial biofuel crops in a variable climate. *GCB Bioenergy* **2015**, *7* (6), 1344−1356.
(23) Hamilton, S. K.; Hussain, M. Z.; Bhardwaj, A. K.; Basso, B.; Robertson, G. P. Comparative water use by maize, perennial crops, restored prairie, and poplar trees in the US Midwest. *Environ. Res. Lett.* **2015**, *10* (6), 064015.
(24) Davis, M. P.; David, M. B.; Voigt, T. B.; Mitchell, C. A. Effect of nitrogen addition on Miscanthus × giganteus yield, nitrogen losses, and soil organic matter across five sites. *GCB Bioenergy* **2015**, *7* (6), 1222−1231.
(25) Nyakatawa, E. Z.; Mays, D. A.; Tolbert, V. R.; Green, T. H.; Bingham, L. Runoff, sediment, nitrogen, and phosphorus losses from agricultural land converted to sweetgum and switchgrass bioenergy feedstock production in north Alabama. *Biomass Bioenergy* **2006**, *30* (7), 655−664.
(26) Smith, C. M.; David, M. B.; Mitchell, C. A.; Masters, M. D.; Anderson-Teixeira, K. J.; Bernacchi, C. J.; DeLucia, E. H. Reduced Nitrogen Losses after Conversion of Row Crop Agriculture to Perennial Biofuel Crops. *J. Environ. Qual.* **2013**, *42* (1), 219−228.
(27) Ng, T. L.; Eheart, W. J.; Cai, X.; Miguez, F. Modeling Miscanthus in the Soil and Water Assessment Tool (SWAT) to Simulate Its Water Quality Effects As a Bioenergy Crop. *Environ. Sci. Technol.* **2010**, *44* (18), 7138−7144.
(28) Baskaran, L.; Jager, H. I.; Schweizer, P. E.; Srinivasan, R. Progress toward Evaluating the Sustainability of Switchgrass as a Bioenergy Crop using the SWAT Model. *Trans. ASABE* **2010**, *53* (5), 1547−1556.
(29) Wu, Y.; Liu, S. Impacts of biofuels production alternatives on water quantity and quality in the Iowa River Basin. *Biomass Bioenergy* **2012**, *36*, 182−191.
(30) Wu, Y.; Liu, S.; Li, Z. Identifying potential areas for biofuel production and evaluating the environmental effects: a case study of the James River Basin in the Midwestern United States. *GCB Bioenergy* **2012**, *4* (6), 875−888.
(31) Wu, Y.; Liu, S.; Sohl, T. L.; Young, C. J. Projecting the land cover change and its environmental impacts in the Cedar River Basin in the Midwestern United States. *Environ. Res. Lett.* **2013**, *8* (2), 024025.
(32) Davis, S. C.; Parton, W. J.; Del Grosso, S. J.; Keough, C.; Marx, E.; Adler, P. R.; DeLucia, E. H. Impact of second-generation biofuel agriculture on greenhouse-gas emissions in the corn-growing regions of the US. *Front. Ecol. Environ.* **2012**, *10* (2), 69−74.
(33) Stone, K. C.; Hunt, P. G.; Cantrell, K. B.; Ro, K. S. The potential impacts of biomass feedstock production on water resource availability. *Bioresour. Technol.* **2010**, *101* (6), 2014−2025.
(34) VanLoocke, A.; Twine, T. E.; Zeri, M.; Bernacchi, C. J. A regional comparison of water use efficiency for miscanthus, switchgrass and maize. *Agri. For. Meteorol.* **2012**, *164*, 82−95.
(35) Yaeger, M. A.; Housh, M.; Cai, X.; Sivapalan, M. An integrated modeling framework for exploring flow regime and water quality changes with increasing biofuel crop production in the U.S. Corn Belt. *Water Resour. Res.* **2014**, *50* (12), 9385−9404.
(36) Qin, Z.; Zhuang, Q. Estimating Water Use Efficiency in Bioenergy Ecosystems Using a Process-Based Model. In *Remote Sensing of the Terrestrial Water Cycle*; Lakshmi, V., Eds.; John Wiley & Sons, Inc., 2014; pp 479−491.
(37) Breshears, D. D.; Barnes, F. J. Interrelationships between plant functional types and soil moisture heterogeneity for semiarid landscapes within the grassland/forest continuum: a unified conceptual model. *Landscape Ecol.* **1999**, *14*, 465−478.
(38) Asbjornsen, H.; Goldsmith, G. R.; Alvarado-Barrientos, M. S.; Rebel, K.; Van Osch, F. P.; Rietkerk, M.; Chen, J.; Gotsch, S.; Tobon, C.; Geissert, D. R.; et al. Ecohydrological advances and applications in plant-water relations research: a review. *J. Plant Ecol.* **2011**, *4* (1−2), 3−22.
(39) Barney, J. N.; Mann, J. J.; Kyser, G. B.; Blumwald, E.; Van Deynze, A.; DiTomaso, J. M. Tolerance of switchgrass to extreme soil moisture stress: Ecological implications. *Plant Sci.* **2009**, *177* (6), 724−732.
(40) Zhang, X.; Izaurralde, C. R.; Arnold, J. G.; Sammons, N. B.; Manowitz, D. H.; Thomson, A. M.; Williams, J. R. Comment on 'Modeling Miscanthus in the Soil and Water Assessment Tool (SWAT) to Simulate Its Water Quality Effects As a Bioenergy Crop'. *Environ. Sci. Technol.* **2011**, *45* (14), 6211−6212.
(41) Jain, A.; Yang, X.; Kheshgi, H.; McGuire, D. A.; Post, W.; Kicklighter, D. Nitrogen attenuation of terrestrial carbon cycle response to global environmental factors. *Global Biogeochem. Cy.* **2009**, *23* (4), GB4028 1−13..
(42) Yang, X.; Wittig, V.; Jain, A. K.; Post, W. Integration of nitrogen cycle dynamics into the Integrated Science Assessment Model for the study of terrestrial ecosystem responses to global change. *Global Biogeochem. Cy.* **2009**, *23* (4), GB4029 1−18..
(43) Song, Y.; Jain, A. K.; McIsaac, G. F. Implementation of dynamic crop growth processes into a land surface model: evaluation of energy, water and carbon fluxes under corn and soybean rotation. *Biogeosciences* **2013**, *10*, 8039−8066.
(44) Barman, R.; Jain, A. K.; Liang, M. Climate-driven uncertainties in modeling terrestrial gross primary production: a site level to global-scale analysis. *Global Change Biol.* **2014a**, *20* (5), 1394−1411.
(45) Barman, R.; Jain, A. K.; Liang, M. Climate-driven uncertainties in modeling terrestrial energy and water fluxes: a site-level to global-scale analysis. *Global Change Biol.* **2014b**, *20* (6), 1885−1900.
(46) Meiyappan, P.; Jain, A. K. Three distinct global estimates of historical land-cover change and land-use conversions for over 200 years. *Front. Earth Sci.* **2012**, *6* (2), 122−139.
(47) Klein Goldewijk, K.; Beusen, A.; Van Drecht, G.; De Vos, M. The HYDE 3.1 spatially explicit database of human-induced global land-use change over the past 12,000 years. *Glob. Ecol. Biogeogr. Lett.* **2011**, *20* (1), 73−86.
(48) Miller, D. A.; White, R. A. A Conterminous United States Multilayer Soil Characteristics Dataset for Regional Climate and Hydrology Modeling. *Earth Interact.* **1998**, *2* (1), 2−2.
(49) Liu, Q. *Land surface modeling with enhanced considerations of soil hydraulic properties and terrestrial ecosystems*. Ph. D. Dissertation, Georgia Institute of Technology, Atlanta, GA, 2003.
(50) *Breaking the Biological Barriers to Cellulosic Ethanol: A Joint Research Agenda; DOE/SC-0095*; U.S. Department of Energy Office of Science and Office of Energy Efficiency and Renewable Energy: Rockville, MD, 2006; http://genomicscience.energy.gov/biofuels/-2005workshop/b2blowres63006.pdf.

DOI: 10.1021/acs.est.5b05239
Environ. Sci. Technol. XXXX, XXX, XXX−XXX

(51) Cadoux, S.; Riche, A. B.; Yates, N. E.; Machet, J.-M. Nutrient requirements of Miscanthus x giganteus: Conclusions from a review of published studies. *Biomass Bioenergy* **2012**, *38*, 14−22.
(52) Jach-Smith, L. C.; Jackson, R. D. Nitrogen conservation decreases with fertilizer addition in two perennial grass cropping systems for bioenergy. *Agric., Ecosyst. Environ.* **2015**, *204*, 62−71.
(53) Mitchell, K. E.; Lohmann, D. L.; Houser, P. R.; Wood, E. F.; Schaake, J. C.; Robock, A.; Cosgrove, B. A.; Sheffield, J.; Duan, Q.; Luo, L.; et al. The multi-institution North American Land Data Assimilation System (NLDAS): Utilizing multiple GCIP products and partners in a continental distributed hydrological modeling system. *J. Geophys. Res.* **2004**, *109* (7), D07S90 1−32..
(54) Soil Survey Staff; Natural Resources Conservation Service, United States Department of Agriculture. Web Soil Survey. http://websoilsurvey.nrcs.usda.-gov/.
(55) Zeng, N. Seasonal cycle and interannual variability in the Amazon hydrologic cycle. *J. Geophys. Res.* **1999**, *104* (D8), 9097−9106.
(56) Arundale, R. A.; Dohleman, F. G.; Voigt, T. B.; Long, S. P. Nitrogen Fertilization Does Significantly Increase Yields of Stands of Miscanthus × giganteus and Panicum virgatum in Multiyear Trials in Illinois. *BioEnergy Res.* **2014**, *7* (1), 408−416.
(57) Dohleman, F. G.; Heaton, E. A.; Leakey, A. D. B.; Long, S. P. Does greater leaf-level photosynthesis explain the larger solar energy conversion efficiency of Miscanthus relative to switchgrass? *Plant, Cell Environ.* **2009**, *32* (11), 1525−1537.
(58) Anderson-Teixeira, K. J.; Masters, M. D.; Black, C. K.; Zeri, M.; Hussain, M. Z.; Bernacchi, C. J.; DeLucia, E. H. Altered Belowground Carbon Cycling Following Land-Use Change to Perennial Bioenergy Crops. *Ecosystems* **2013**, *16* (3), 508−520.
(59) Ma, Z.; Wood, C. W.; Bransby, D. I. Impacts of soil management on root characteristics of switchgrass. *Biomass Bioenergy* **2000**, *18* (2), 105−112.
(60) Kaisi, M. M. Al-; Grote, J. B. Cropping Systems Effects on Improving Soil Carbon Stocks of Exposed Subsoil. *Soil Sci. Soc. Am. J.* **2007**, *71* (4), 1381.
(61) Ontl, T. A.; Hofmockel, K. S.; Cambardella, C. A.; Schulte, L. A.; Kolka, R. K. Topographic and soil influences on root productivity of three bioenergy cropping systems. *New Phytol.* **2013**, *199* (3), 727−737.
(62) Owens, V. N.; Viands, D. R.; Mayton, H. S.; Fike, J. H.; Farris, R.; Heaton, E.; Bransby, D. I.; Hong, C. O. Nitrogen use in switchgrass grown for bioenergy across the USA. *Biomass Bioenergy* **2013**, *58*, 286−293.
(63) Woo, D. K.; Quijano, J. C.; Kumar, P.; Chaoka, S.; Bernacchi, C. J. Threshold Dynamics in Soil Carbon Storage for Bioenergy Crops. *Environ. Sci. Technol.* **2014**, *48* (20), 12090−12098.
(64) Bala, G.; Caldeira, K.; Wickett, M.; Phillips, T. J.; Lobell, D. B.; Delire, C.; Mirin, A. Combined climate and carbon-cycle effects of large-scale deforestation. *Proc. Natl. Acad. Sci. U. S. A.* **2007**, *104* (16), 6550−6555.
(65) Hallgren, W.; Schlosser, C. A.; Monier, E.; Kicklighter, D.; Sokolov, A.; Melillo, J. Climate impacts of a large-scale biofuels expansion.Geophysical. *Res. Lett.* **2013**, *40* (8), 1624−1630.
(66) Georgescu, M.; Lobell, D. B.; Field, C. B. Direct climate effects of perennial bioenergy crops in the United States. *Proc. Natl. Acad. Sci. U. S. A.* **2011**, *108* (11), 4307−4312.

DOI: 10.1021/acs.est.5b05239
Environ. Sci. Technol. XXXX, XXX, XXX−XXX